8.4 MOMENTUM FLUXES AND TURBULENCE STRUCTURE OF THE MARINE ATMOSPHERIC BOUNDARY LAYER

Costas G. Helmis[1], George Sgouros[1], Christofors H. Halios[1], and Qing Wang[2]
[1]Department of Applied Physics
Faculty of Physics, University of Athens, Greece
[2]Department of Meteorology
Naval Postgraduate School, Monterey, CA, USA

1. INTRODUCTION

The characteristics of the Atmospheric Boundary Layer (ABL) at maritime areas are exhibited strong variations in space and time due to the land/sea surface forcing and the modification of the wind flow field related to terrain and surface thermal effects. The study of coastal ABL has been received considerable attention with respect to the upwind Marine Atmospheric Boundary Layer (MABL), since uncertainties related to the parameterization of the mass, heat and moisture exchange between the air and sea are existed and experimental studies reveal large data scatter and even apparent inconsistencies in results (Gryning and Batchvarova, 2002, Smedman et al., 2004). Also the study of the coastal ABL is of major interest due to the air pollution problems from industrial sites and big cities located in the coastal region (Lalas et al. 1987, Garratt, 1990, Helmis et al. 1997), or wind energy applications (Hogstrom et al, 1988). Moreover, certain atmospheric phenomena such as Low Level Jets (LLJ) or intensified thermal stratifications are associated with the marine ABL (Smedman et al, 1993).

The ability of Acoustic Sounders (SODARS) to measure the mean and the turbulent characteristics of the wind flow as well as the thermal structure of the ABL is well known (Coulter and Kallistratova, 2004, Kallistratova and Coulter, 2004, Helmis et al, 2000). With high temporal and spatial resolution, especially in the vertical direction, it is sometimes more desirable to use them compared to the single-level turbulence measurements in certain research areas of the ABL.

In spite of the wide use of SODARS for atmospheric boundary layer investigations during the last three decades over land (Neff and Coulter 1986, Asimakopoulos et al. 1983), the experience of using these systems have demonstrated the feasibility of SODARS operating over the ocean (Fairall et al, 1997, Petenko et al, 1996), over small island (Helmis et al. 2002) or on the shoreline (Helmis et al. 1987).

Furthermore, estimation of Turbulent Kinetic Energy (TKE) and momentum flux profiles under slightly stable conditions is possible, using the Kolmogorov - Prandtl semi-empirical theory of turbulence, together with simple parameterization under near neutral conditions (Kramar and Kuznetsov, 2002, Kouznetsov et al, 2004).

This work was conducted in the frame of the CBLAST-Low project which was aimed at the understanding of the air-sea interaction and the coupled atmospheric and oceanic boundary layer dynamics at low wind speeds, where the dynamic processes are driven and/or strongly modulated by thermal forcing (Edson et al, 2004). In this experimental study, combining both in situ and remote sensing data, the characteristics of the turbulent vertical structure of the upwind MABL over a maritime area are examined. Also, the development of the LLJ and the turbulent characteristics below and above the LLJ core, under the stability stratification found in the marine environment, are examined and discussed.

2. EXPERIMENTAL AREA AND INSTRUMENTATION

The experimental campaign was carried out during summer 2003 (31st of July to 27th of August) at the Nantucket Island, MA, USA. Our measurement site was at the southerly-westerly coast of the island, at a distance of 90m from the waterfront where the land surface was relatively flat. A suite of in situ and remote sensing instruments designed to characterize the changing structure of the MABL was deployed. A SODAR system was measuring the vertical profiles of the horizontal wind speed and direction, the echo strength, the vertical (w) and the two horizontal wind components u (north-westward) and v (north-eastward), the standard deviations of the three wind components, the momentum fluxes ($u'w'$ and $v'w'$) and the atmospheric static stability class at 30 minutes intervals, with a vertical resolution of 40m and a range up to the height of 600m. The total vertical momentum fluxes and the TKE were also calculated. More details regarding SODAR system and its parameters can be found at Helmis et al. (2004). On a 20m meteorological mast, there were two levels (10 and 20m) of high-rate sampling sonic anemometers, a fast hygrometer at 20m and slow response sensors measuring the mean wind, temperature, and relative humidity at 5, 10, and 20m

---

Corresponding author address: Costas G. Helmis, University of Athens, Department of Applied Physics, University Campus, Building Phys.-5, 15784, Athens, GREECE, e-mail: chelmis@cc.uoa.gr

height respectively at 10 minutes intervals with a sampling frequency of 1Hz (Wang et al. 2004). The high-rate measurements (20Hz) yield to the estimation of momentum, sensible heat and latent heat fluxes through the eddy correlation method. It should be mentioned that the values of momentum, heat and humidity fluxes and the stability parameter z/L, calculated at 20m height by the fast sensors, were used as reference surface values of the MABL, while the 10m height ones were excluded from this study since they were influenced by the developed Internal Boundary Layer (IBL). In addition, rawinsondes were launched at the experimental site every four to six hours per day.

3. RESULTS AND DISCUSSION

In order to study the turbulence structure of the MABL, under different meteorological conditions, experimental data for the 7th and the 3rd of August 2003 are presented and discussed.

3.1 *The 7th of August 2003*

In Figures 1 and 2 the mean sea level pressure fields with IR satellite images and weather observations and the 500 hPa geopotential distribution respectively at 12:00 UTC are presented.

The area of Nantucket was under the influence of a frontal depression, located just ahead of the eastward advancing cold front (Figure 1), while a large scale anticyclone prevailed over the greater Northern Atlantic area. Therefore, an intense surface southerly/south-westerly flow of 12 to 14 m/sec was established over the island accompanied with cloudy conditions and scattered rainfall during the morning and afternoon hours. A large scale trough advanced towards the island at the upper levels at 500 hPa, producing strong south-westerly flow up to 3km height during all day with moderate to high wind speed (Figure 2).

Figure 3 gives the vertical profiles of the horizontal wind speed and the wind direction, estimated by three successive radiosonde launches at 05:48, 18:00 and 24:00 UTC respectively during the experimental day. Conversion from UTC to LST requires a subtraction of 4 hours (LST = UTC - 4hr). The wind direction is almost constant up to 1000m height from the south – southwesterly sector (200-220 degrees). At the wind speed profiles the development and preservation of a LLJ into a relatively shallow layer (about 50m) between 200m and 250m height with high wind speed (13 m/sec) is evident.

Figure 4 gives the vertical profiles of the potential temperature and the relative humidity for the same time periods. The potential temperature profiles show a very stable surface layer (with mean potential temperature gradient $\Delta\theta/\Delta z = 2^{o}K/100m$) extending up to 200m height and a slightly stable layer (with gradient $\Delta\theta/\Delta z = 0.4^{o}K/100m$) at higher levels up to 1000m height. It should be mentioned that all temperature profiles were characterized by inversion layers at heights between 350 and 500m while during the third launching the ground based inversion was limited to 140m.

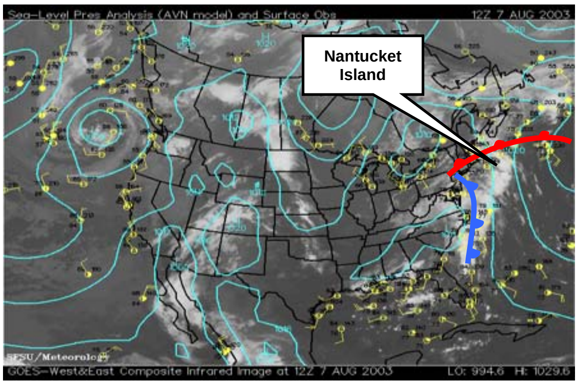

Fig.1: Mean Sea level pressure fields with IR satellite image and weather observations for 7/8/2003 12:00 UTC (Source: California Regional Weather Server).

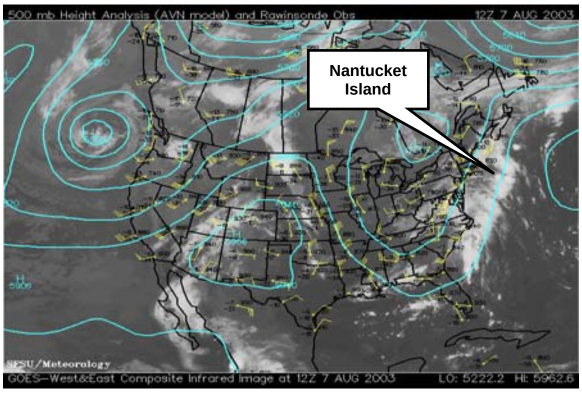

Fig. 2: 500 hPa geopotential distribution with IR satellite image for 7/8/2003 12:00 UTC (Source: California Regional Weather Server)

The corresponding relative humidity profiles give a surface layer with high values (more than 95%) at the first 100m, then a gradually decrease at the next 100m followed by a layer (between 200 and 400m) characterized by almost constant humidity in the range of 85-90%. Intense relative humidity gradients were also observed at the layer between 400-500m while at higher levels the relative humidity values remain high due to cloudiness that occurred during almost the whole day. It is interesting to note that the LLJ is observed on the top of the intense ground based temperature inversion. According to the literature, the development as well as the characteristics of the marine LLJ have been observed and studied from various researchers under different conditions. It was found that a large scale horizontal temperature contrast causing baroclinicity in the ABL (Gerber et al., 1989 and Li et al. 1983) or an inertial oscillation due to frictional decoupling over the sea (Smedman et al. 1995), are possible causes of the LLJ development. In our case, where a very stable stratification characterizes the lower part of the ABL, the main mechanism is likely to be the frictional decoupling and the subsequent inertial oscillation, although horizontal temperature gradients possibly existed (more discussion on this at the end of this section).

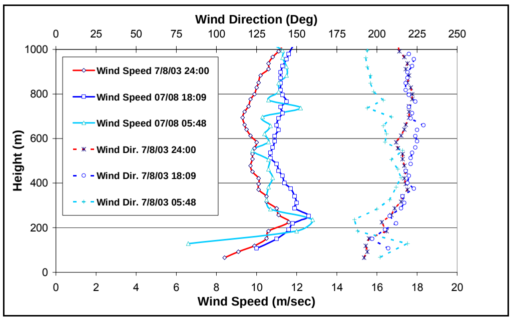

Fig. 3: Horizontal Wind Speed and Direction profiles measured by the radiosonde for 7/8/2003.

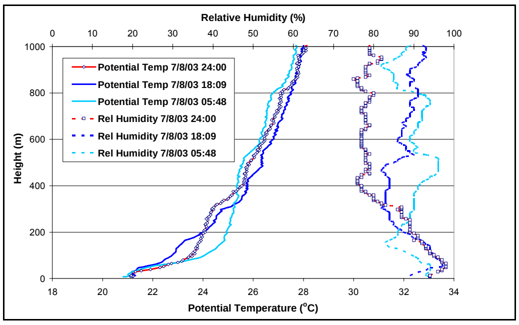

Fig. 4: Potential Temperature and Relative Humidity profiles measured by the radiosonde for 7/8/2003.

Figure 5 gives the time-height cross sections of the wind speed vectors estimated by the SODAR during the period between 12:30 to 23:30 UTC of this day. The constant south-westerly wind field with moderate to high wind speed is characterizing the whole day.

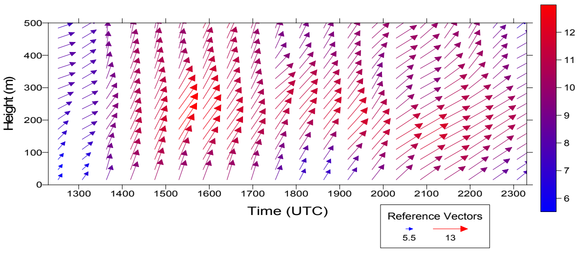

Fig. 5: Time-height cross section of the wind vectors (m/sec) during 7/8/2003 12:30 – 23:30 UTC.

The time-height cross section of the wind speed estimated by the SODAR is given in Figure 6. This contour plot also includes the sonic anemometer's measurement at the height of 20m. During the period from 14:00 UTC to 17:00 UTC the evolution of a LLJ at the height of 200-250m is evident, which is gradually descending to the height of 100-150m between 19:00 to 22:00 UTC, while its strength is decreasing slightly. The ABL up to the first 80m is characterized by intense wind speed shear, which is more intense when the LLJ is present.

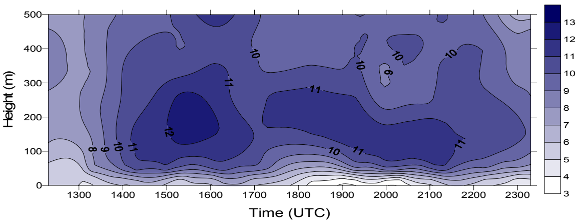

Fig. 6: Time-height cross section of the wind speed (m/sec) during 7/8/2003 12:30 – 23:30 UTC, including the sonic anemometer's measurement at 20m.

Figure 7 gives the atmospheric stability class derived from the SODAR for the same period. Stability classes 1, 2 and 3 correspond to stable, slightly stable and neutral stratification respectively. Stable to neutral conditions characterize the vertical structure of the MABL. For a time period of about 3 hours (14:00 – 17:00 UTC) and under the presence of the LLJ, neutral conditions are evident for the layer above its core, while slightly stable to more stable conditions are observed below the LLJ. The break up of the LLJ (after 22:00 UTC) is accompanied with an increased stability at higher levels.

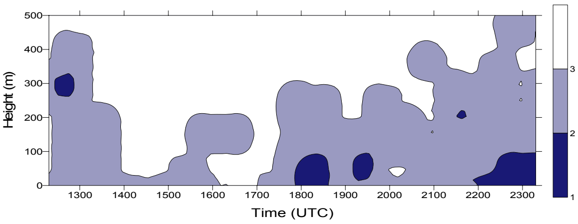

Fig. 7: Time-height cross-section of the atmospheric stability during 7/8/2003 12:30 – 23:30 UTC. Stability classes are given in the text.

At Figure 8 the time-height plot of the echo strength (analogue to the temperature structure parameter C_T^2) in arbitrary units calculated by the SODAR for the same period is presented. A strong echo maximum (corresponding to areas where strong temperature or humidity gradients exist) is established at 350 – 500m height almost for the whole time period. According to the radiosonde soundings (see Fig. 4) this height is characterized by strong humidity and temperature gradients, which are persistent during the day. A secondary maximum is evident at the height of 150 to 200m (especially at 19:00 UTC when it is strengthening) that is corresponding to the top of the surface ground based inversion with strong stability observed by the radiosondes.

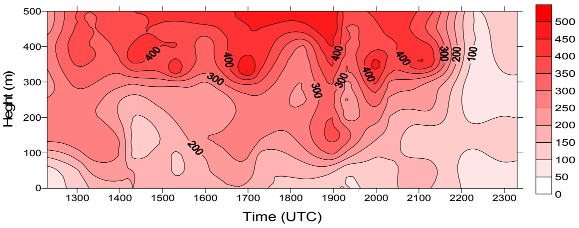

Fig. 8: Time-height cross section of the echo strength (arbitrary units) during 7/8/2003 12:30 – 23:30 UTC.

At Figure 9 the Total Vertical Momentum Flux, the sum of the momentum fluxes $\left(\left(\overline{u'w'}\right)^2+\left(\overline{v'w'}\right)^2\right)^{1/2}$ calculated by the SODAR is presented. The profiles of the total vertical momentum fluxes give high values above the wind maximum height and much lower ones close to the surface, which are associated with the evolution of the LLJ.

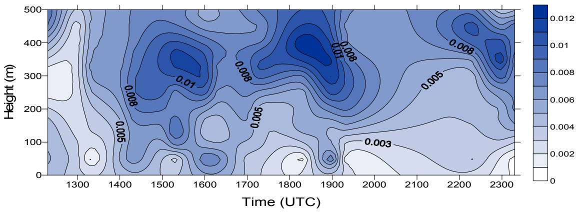

Fig. 9: Time-height cross section of the Total Vertical Momentum Flux during 7/8/2003 12:30 – 23:30 UTC.

Figure 10 gives the time-height plot of the TKE calculated by the SODAR for the same period. According to Kouznetsov et al (2004) the TKE can be derived, under neutral stratification, from the variance of the vertical wind component ($\sigma^2 w$) using the relation $TKE \cong 3.4\ \sigma_w^2$ in the SODAR-covered part of the ABL, while under non-neutral conditions the coefficient of the relation should be a function of M-O stability parameter z/L. Large values of the TKE exist at heights above the LLJ, which is probably associated with the shear forcing near the developed wind maximum, while secondary maximum with lower values are observed below the LLJ layer. It seems that close to the surface, even though the wind speed shear is much more intense than at higher levels, the increased stability at the surface layer restrains the turbulence.

Finally, Figure 11 gives the horizontal wind speed hodograph derived by the SODAR data for the time period between 11:00 UTC of the 7th of August to 03:00 UTC for the next day at the level of 250m height. A wind vector oscillation is evident, with a period of about 15 hours.

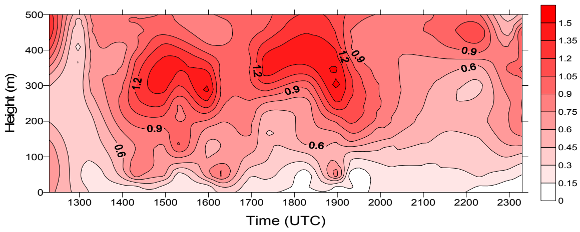

Fig. 10: Time-height cross section of the Turbulent Kinetic Energy (TKE) during 7/8/2003 12:30 – 23:30 UTC.

The LLJ is present for almost 7 hours from 15:00 till 22:00 UTC of the 7th of August. This behavior is in agreement with the plausible explanation that the cause for the development of the LLJ, which is associated with a strong stability of the MABL lower layer, is the development of an inertial oscillation due to the frictional decoupling over the sea (Smedman et al., 1993, 1997).

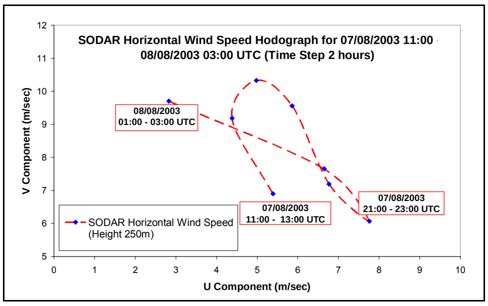

Fig. 11: Horizontal Wind Speed Hodograph (time step: 2h, height: 250m) for the time period 7/8/2003 11:00 – 8/8/2003 03:00 UTC

3.2 *The 3rd of August 2003*

According to the synoptic maps (not shown here) during this day, the greater area of Nantucket was influenced by the passage of a frontal depression. More specifically, the island was inside the warm sector at the edge of a northward advancing warm front. An intense surface southerly/south-westerly flow of 12 to 13 m/sec was established over the island under fair conditions, being accompanied by warm air advection towards the island. At higher levels, a large scale trough advancing towards the island was located above the north-eastern part of the USA. This trough produced strong southerly-westerly flow, while anticyclonic conditions prevailed over the island.

Figure 12 presents the wind speed and direction profiles estimated by two successive radiosondes launches at 12:55 and 18:32 UTC of this day. The corresponding Potential Temperature and Relative Humidity profiles for the same period are shown at Figure 13. According to these figures the wind direction was kept constant at 240 degrees (south-westerly flow) for a relatively deep layer at the first 1500m, while intense LLJ (with values 11,5m/sec) was observed at the height of 190m (at 12:55 UTC) that was strengthened to 12m/sec and was gradually descended to 150m (at 18:32 UTC). The Potential temperature profiles exhibited a strong surface based inversion (about 2^{o}K/100m, see figure 13) up to 160m height associated with strong relative humidity values (close to 95%). At higher levels the atmosphere was less stable with an intense inversion layer at 700m height. It should be mentioned that the LLJ was developed again on the top of the surface inversion layer.

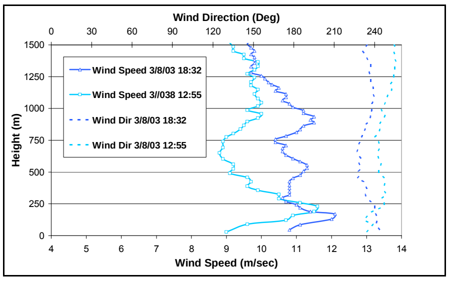

Fig. 12: Horizontal Wind Speed and Direction profiles measured by the radiosonde for 3/8/2003.

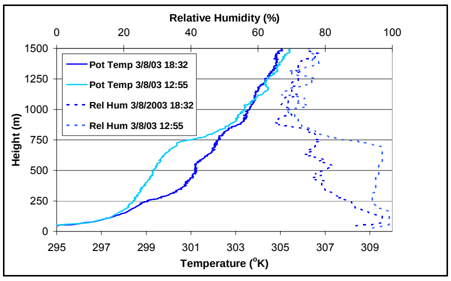

Fig. 13: Potential Temperature and Relative Humidity profiles measured by the radiosonde for 3/8/2003.

The time-height cross section of the wind speed estimated by the SODAR for the period 11:00 – 20:00 UTC of this day is presented in Figure 14. After 11:00 UTC a LLJ is observed at the height of about 200m into a shallow layer (less than 100m). During the period 17:00 to 20:00 UTC the LLJ is gradually strengthening and is descending to the height of 150m (in accordance with the radiosonde observations).

The atmospheric stability derived by the SODAR (Figure 15) shows slightly stable conditions up to about 400m, with the exception of the periods between 13:00 to 15:00 UTC and 16:00 to 18:00 UTC where a very stable surface layer is present associated with the LLJ strengthening. At higher levels (above the LLJ core) slightly stable to neutral conditions exist.

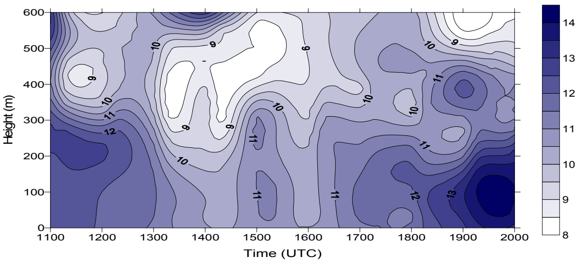

Fig. 14: Time-height cross section of the wind speed (m/sec) during 3/8/2003 11:00 – 20:00 UTC.

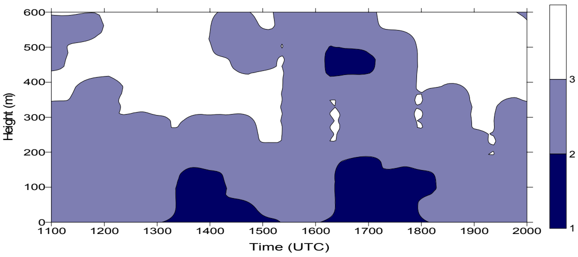

Fig. 15: Time-height cross section of the atmospheric stability during 3/8/2003 11:00 – 20:00 UTC.

The horizontal wind speed hodograph derived by the SODAR data for the period of 00:00 – 16:00 UTC, of the 3rd of August, for the level of 230m, is shown at Figure 16. A very well defined oscillation of the wind speed vectors is evident with a period of almost 16 hours. This fact is strengthening the suggestion that the inertial oscillation due to frictional decoupling is the main possible mechanism for the generation of the LLJ. The observed LLJ persists for about 6 to 7 hours exhibiting relatively high wind speeds, while performing a directional shift. During the LLJ development the wind vectors shift to more westerly wind directions.

Figures 17 and 18 give the time-height plot of the total vertical momentum flux and the TKE calculated by the SODAR for the same period. The TKE profiles exhibit high values above the LLJ core, associated with near neutral conditions while lower values are observed below the LLJ layer. The total vertical momentum flux profiles show the same characteristics as the previously described experimental day.

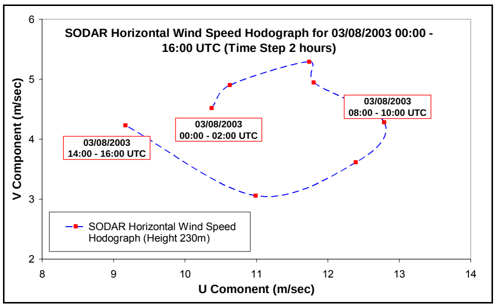

Fig. 16: Horizontal Wind Speed Hodograph (time step: 2h, height: 230m) for the time period 3/8/2003 00:00 – 16:00 UTC.

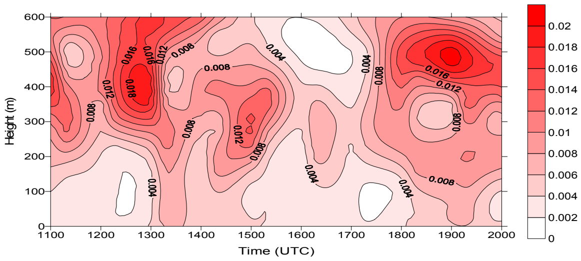

Fig. 17: Time-height cross section of the Total Vertical Momentum Flux during 3/8/2003 11:00 – 20:00 UTC.

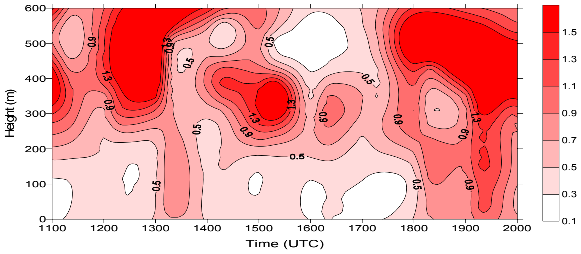

Fig. 18: Time-height cross section of the Turbulent Kinetic Energy (TKE) during 3/8/2003 11:00 – 20:00 UTC.

4. CONCLUDING REMARKS

The analysis of the measurements using both in-situ and remote instrumentation, revealed the characteristics of the mean and turbulent vertical structure of the MABL near the coast of an island. Study of the vertical profiles of the echo strength (analogue to the temperature structure parameter CT_2) and stability class from the SODAR data has shown that the MABL is characterized by very stable atmospheric conditions at the lowest 150-200m followed by slight stable to neutral conditions at higher levels.

It was observed, very frequently, under medium to high wind speeds, the development of a Low-Level Jet (LLJ) with a maximum corresponding to the top of the surface based stable layer. The estimated profiles of the potential temperature, specific humidity, wind speed and direction, from the rawinsondes launches, confirmed the mentioned above vertical structure of the MABL, where the intense ground based inversion, the different layering above and the developed LLJ were also observed. A possible cause for the development of the LLJ, which is associated with the strong stability of the MABL lower layer, is the development of an inertial oscillation due to the frictional decoupling over the sea. This plausible explanation is in agreement with the calculated hodographs of the wind vector, estimated from SODAR data at the LLJ core layer, where the relative increase of the wind speed and the wind direction turning were evident. The estimated profiles of the total vertical momentum fluxes give high values above the wind maximum height and much lower ones close to the surface. Large values of the TKE exist above the LLJ core layer, which are probably associated with the shear forcing near the developed wind maximum, while secondary maximum with lower values are observed below the LLJ layer. It is interesting to note that close to the surface, even though the wind speed shear is much more intense than at higher levels, the increased stability at the surface layer restrains the turbulence.

5. ACKNOWLEDGEMENTS

This work was supported by the Office of Naval Research (Contract No N62558-03-M-0532 and its supplemental award N62558-04-P-6010).

6. REFERENCES

Asimakopoulos D.N., Moulsley T.J., Helmis C.G., Lalas D.P. and Gaynor J., 1983: Quantitative low level acoustic Sounding and comparison with direct measurements, *Boundary Layer Meteorology*, **27**, 1-26.

Coulter, R.L., and Kallistratova, M.A., 2004: Two decades of progress in SODAR techniques: a review of 11 ISARS *Proceedings. Meteorol. Atmos. Phys*., Vol **85**, No 1-3, 3-20.

Edson J., Crofoot R., McGillis W., Zappa C., 2004: Investigations of flux-profile relationships in the marine atmospheric surface layer during CBLAST. *16th Symposium on Boundary Layers and Turbulence,* 9-14 August 2004, Portland, ME.

Fairall CW, White AB, Edson JB, Hare JE, 1997: Integrated shipboard measurements of the marine boundary layer, *Journal of Atmo. Ocea. Technology*, **14**(3), 338-359.

Garratt JR., 1990 : The internal boundary layer: a review. *Boundary Layer Meteorology*, **50**, 171-203.

Gerber, H., Chanf, S. and Holt, T., 1989: Evolution of a Marine Boundary Layer Jet. J. Atm. Sci., 46, 1312 – 1326.

Gryning SE., Batchvarova E., 2002: Marine Boundary layer and turbulent fluxes over the Baltic sea:

measurements and modeling. Boundary Layer Meteorology, 103, 92-47.

Helmis C.G., Q. Wang, C.H. Halios, S.W. Wang and G. Sgouros, 2004: On the vertical turbulent structure of the Marine Atmospheric Boundary Layer, *16th Symposium of the AMS on Boundary Layers and Turbulence,* Portland, ME, 9-13 August.

Helmis CG, Jacovides C, Asimakopoulos DN and Flocas HA, (2002): Experimental study of the vertical structure of the lower troposphere over a small Greek island in the Aegean Sea, *Journal of Atmospheric Ocean. Tech.,* **19**(8), 1181-1192.

Helmis C.G., Kalogiros J.A., Assimakopoulos D.N. and Soilemes A.T., 2000: Estimation of potential temperature gradient in turbulent stable layers using Acoustic Sounder Measurements. *Quarterly Journal of the Royal Meteological Society*, **126**, pp 31 – 61.

Helmis C.G., Tombrou M., Asimakopoulos D.N., Soilemes A., Gósten H., Moussiopoulos N.and Hazaridou A.,1997: "Thessaloniki '91 Field Measurement Campaign; Part I: Wind field and Atmospheric Boundary Layer structure over the Greater Thessaloniki Area under light background flow", *Atmospheric Environment*, **31**, 8, 1101 -1114.

Helmis C.G., Asimakopoulos D.N., Deligiorgi D.G. and Lalas D.P., 1987: Observations of the sea-breeze front structure near the shoreline, *Boundary Layer Meteorology*, **38**, 395-410.

Hogstrom U., Asimakopoulos D. N., Kambezidis H., Helmis C.G. and Smedman A., 1988: A field study of the wake behind a 2 MW wind turbine. *Atmospheric Environment*, **22**, 803 – 820.

Kallistratova, M.A., and Coulter, R.L., 2004: Application of SODARs in the study and monitoring of the environment. *Meteorol. Atmos. Phys*., **85**, No 1-3, 21-38.

Kouznetsov RD, Kramar VF, Beyrich F and Engelbart D (2004): SODAR-based estimation of TKE and momentum flux profiles in the atmospheric boundary layer: Test of a parameterization model, *Meteorol. Atmos. Phys*., **85** (1-3): 93-99.

Kramar VF, Kouznetsov RD, (2002), ‘A new concept for estimation of turbulent parameter profiles in the ABL using sodar data’, J Atmos Ocean Tech, 19(8), 1216-1224.

Lalas D.P., Tombrou-Tsella M., Petrakis M., Asimakopoulos D.N. and Helmis C.G., 1987: "An experimental study of horizontal and vertical distribution of ozone over Athens", *Atmospheric Environment*, **21**, 2681-2693.

Li., X.S., Gaynor, J.E. and Kaimal, J.C., 1983: A study of multiple stable layers in the nocturnal lower atmosphere. *Boundary Layer Meteorology*. **26**, 157 – 167.

Neff W.D. and R.L. Coulter, 1986: “Acoustic Remote Sensing”, Probing the Atmospheric Boundary Layer, D.H. Lenschow, Editor, American Meteorological Society, PP 201-266.

Petenko IV, Bedulin AN and Shyrygin YA, (1996) ‘Sodar observations of the atmospheric boundary layer over the ocean during ASTEX-91’, Boundary Layer Meteorology, 81 (1), 63-73.

Smedman AS, Hogstrom U., Larsen G., Johanson C., Rutgersson A., Sjöblom A., Kahma K. K. and Pettersson H., 2004: Towards a fundamentally new understanding of the marine atmospheric boundary layer, 16th Symposium on Boundary Layers and Turbulence, 9-14 August 2004, Portland, ME.

Smedman, A.S., Horstrom, U. and Bergstrom, H., 1997. The turbulence regime of a very stable marine airflow with quasi-frictional decoupling. *J. of Geoph. Res.-Oceans.,* **102 (C9),** 21049-21059.

Smedman, A.S., Bergstrom, H. and Horstrom, U., 1995. Spectra, variances and length scales in a marine stable boundary layer dominated by a low level jet. *Bound-Lay Meteorol.,* **76 (3),** 211-232.

Smedman AS, Tjernstrom M., and Hogstrom U., 1993, Analysis of the turbulence structure of a marine low level jet. Boundary Layer Meteorology, 66,105-126.

Wang Q., C.G. Helmis, Z. Gao, J. Kalogiros and S.W. Wang, 2004: “Variations of Boundary Layer Turbulence and mean Structure using synthesized Observations”, 16th Symposium of the AMS on Boundary Layers and Turbulence, Portland, ME, 9-13 August.